RSC Advances

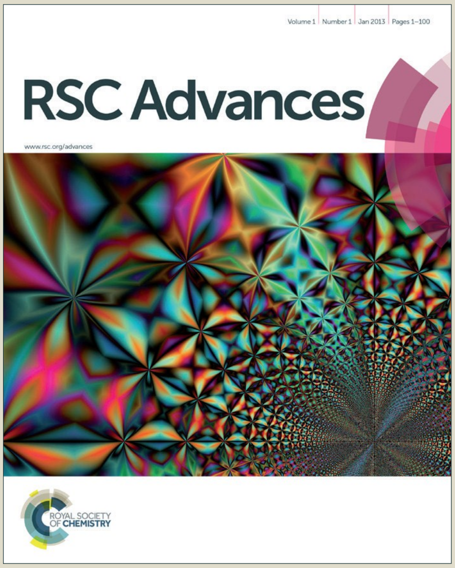

Performance of Al-1Mg-1Zn-0.1Bi-0.02In as anode for Al-AgO battery

Hamed Moghanni-Bavil-Olyaei, Jalal Arjomandi*

Department of Electrochemistry, Faculty of Chemistry, Bu Ali Sina University, 65178 Hamedan, Iran

*To whom correspondence should be addressed, E-mail: j_arjomandi@basu.ac.ir
Tel: +988138288807, Fax: +988138257407

Abstract

In this paper, Al-AgO battery based on Al and Al-1Mg-1Zn-0.1Bi-0.02In (wt%) was prepared and the battery performance was investigated by constant current discharge test in 4 M NaOH and 7 M KOH solutions. The Characterizations of the aluminum anodes after discharge were investigated by electrochemical impedance spectroscopy (EIS). The corrosion behavior of the anodes has been studied using measurements of self-corrosion, potentiodynamic polarization and EIS experiment accompanied with open circuit potential technique and scanning electron microscopy (SEM). The results show that Al-1Mg-1Zn-0.1Bi-0.02In is more active than Al anode, and compared with Al the alloy has the lower self-corrosion rate in both applied electrolyte. It has been observed that the Al-AgO battery based on Al-1Mg-1Zn-0.1Bi-0.02In offers higher operating voltage and anodic utilization than those with Al. At a current density of 50 mA cm^{-2}, the operate voltage of Al-AgO battery is 2.04 V, and the anodic utilization rate is 69.95 % in 7 M KOH solution.

Keywords: Aluminum anode, Al-AgO battery, Battery efficiency, EIS

1. Introduction

Aluminum is used as anode material in Al-AgO because of its negative value of standard electrode potential (-2.35 V vs NHE), high energetic capacity (2980 Ah kg^{-1}), and low weight. The specific energy of Al-AgO battery is 1,090 Wh/kg, which is approximately twice of that of Zn-AgO (540 Wh/kg) [1, 2]. Al-AgO battery having aluminum as anode and divalent silver oxide electrode as cathode with an aqueous sodium hydroxide or potassium hydroxide solution electrolyte is a high performance primary battery [3]. However, practical applications of the Al-AgO battery have been hindered by its low coulombic efficiency caused by the high corrosion rate of aluminum anode in alkaline solutions [4]. Furthermore, presence of natural oxide film on the aluminum delays the activation of it to act as anode and makes aluminum anode potential significantly lower than the theoretical value, thus it needs to be activated to acquire greater power density [5, 6].

To dominate these problems, many researchers confirmed that using extreme purity (99.999 wt%) aluminum doped with elements like In, Mg, Ga, Hg can activate aluminum by omitting or reducing the thickness of oxide film and shift the potential in the direction of more negative value [7-9]. In addition, to reduce the corrosion rate of aluminum anode, the elements of high hydrogen overpotential such as Zn, Bi, Pb, Sn are used [10-12].

The paper has investigated the effect of Bi element on the microstructure and electrochemical properties of Al-Mg-Sn-Ga-Bi alloy [13]. The results of this paper show that Bi in alloy is mainly precipitated along the grain boundaries in the form of segregative phases which are the origins of activation and corrosion of anode alloys in alkaline solutions. Many studies have been done to study the corrosion behavior of Al–Zn–In alloys and detect the activation mechanism of indium and zinc in the alloys [14, 15]. The influences of Zn and In on aluminum activation was elucidated taking into account the displacement reactions that created In accumulation and desirable Zn dissolution [16]. The presence of Mg improves the mechanical properties of aluminum like hardness and strength [17].

This paper describes the electrochemical behavior of Al-Mg-Zn-Bi-In alloy as anode material in Al-AgO battery in 4 M NaOH and 7 M KOH solutions. The aim of this paper is to obtain an alloy of excellent comprehensive electrochemical properties used for Al-AgO battery.

2. Experimental

2.1. Fabrication of electrodes

The nominal compositions of alloy in this experiment are 1 wt.% Mg–1 wt.% Zn–0.1 wt.% Bi–0.02 wt.% In and rest Al. Raw materials are zinc, indium, magnesium, bismuth ingots (>99.9%) and pure aluminum (99.999 wt%) for casting the above anode alloy. The melting process was done in a SiC crucible and using an electrical resistance furnace with a corundum crucible in temperature range of 750-800 ^{o}C. The molten alloy was poured in a preheated cast iron mold. To preparation of AgO cathode, expanded perforated copper sheet as network holder or current collector for active material is prepared. Then it is silver plated to reduce the electrical resistance and to increase the conductivity of electrode grid. A 50 mm × 50 mm × 0.45 mm piece of silver-plated copper grid is served as the current collector. AgO, graphite and Carboxymethyl cellulose (CMC) (typically 90%, 3% and 2% of the final paste weight) are mixed with a mortar and pestle. [It is noteworthy that CMC, as an aqueous dilution of 2-3% and also as a yeast agent, turns the mixture of active electrode materials into a homogeneous dough to provide the possibility of applying that on the surface of electrode grid. It is not considered as a key additive ingredient because it is made to prepare the dough of active materials which are decomposed by heating operation and extracted from electrode tissue. As a result, porosity will be created in the electrode structure]. Then, the appropriate quantity of poly-tetra-fluoro-ethylene (PTFE) suspension is added drop wise and mixed in (PTFE typically 5% of the final past weight). The above mixture is pressed (20 ton in 30 seconds) onto the prepared grid. Eventually, the electrode is allowed to dry at 60°C for 45 min. The resultant AgO cathode is 0.7 mm thick. This fabrication procedure is illustrated in **Fig. 1.**

Fig. 1. here

2.2. Electrochemical measurement

The electrochemical tests (except EIS) were done with three electrodes system at room temperature by potentiostat/galvanostat (Autolab PGSTAT302 N). The EIS measurements were performed by a Zahner/Zennium potentiostat/galvanostat (Zahner, Germany). A saturated calomel electrode (SCE) used as the reference electrode and a rod of graphite was used as the counter electrode. Pure Aluminum and fabricated alloy electrodes with above mentioned composition was utilized as a working electrode (WE). These electrodes were prepared from cubic aluminum, it was mounted in polyester, and so only their cross section (0.93 and 1.33 cm^2 for pure aluminum and alloy, respectively) was allowed to contact the electrolytes. The samples were abraded with emery paper (400 until 2000 grade) and then rinsed with double distilled water. The polarization was measured at a scan rate of 5 mV s^{-1} after OCP measurement. The EIS measurements were done at open circuit potential with a 10 mV AC modulation amplitude in the frequency range of 100 kHz to 100 mHz.

2.3. Self-corrosion

The aluminum specimen (1 × 0.9 × 0.5 cm^3 and 1 × 1.25 × 0.5 cm^3 for pure aluminum and alloy, respectively) were ground with different grades of emery papers, cleaned with acetone, rinsed with distilled water and dried by hair drier and immersed in 4 M NaOH and 7 M KOH solutions for 1 h. The weight of the samples before and after immersion was measured after cleaning the corrosion products formed on the sample surface accurately by a high sensitive balance. The corrosion products were remove in solutions of 2% CrO_3 and 5% H_3PO_4 at 80 °C for about 5 min, then rinsed by distilled water and ethanol. The samples morphology after immersion for 1 h was investigated by JSM-840A scanning electron microscope (SEM) equipped with energy dispersive X-ray (EDX) analysis to identify various precipitates.

The corrosion rate was calculated by the following equation:

$$\text{Corrosion rate (mmpy)} = \frac{87.6\,\Delta W}{DAT}$$

Where ΔW is the weight loss (mg), D is the density ($g.cm^{-3}$), A is the surface area in (cm^2), T is the time (h) and the numeral of 87.6 is from the conversion of hour to year, (mg) to (g) and (cm) to (mm).

2.4. Battery test

The batteries comprised of anode, cathode and electrolyte, where anodes are Al and Al−1Mg−1Zn−0.1Bi−0.02In, cathode is AgO electrode, and electrolytes are 4 M NaOH and 7 M KOH solutions. The discharge performance of Al−AgO batteries was examined by means of constant current discharge test at current densities of 50 mA cm^{-2} for a duration of 20 min. The weight of anode used up was estimated from the weight loss of the anodes during discharge.

The anode utilization was computed using the formula:

$$\text{Anode utilization } \eta = I_{\text{discharge}}\, h / (\Delta W\, F/9.0)$$

Where η is the anode utilization, %; $I_{discharge}$ the discharge current of anode, A; ΔW the weight loss, g; F the faraday constant, h the time, s.

3. Results and discussion

3.1. Open-circuit potential (OCP) and Potentiodynamic polarization (Tafel)

Fig. 2 and **Table 1** show the open-circuit potential vs time curves and self-corrosion rate of Al and Al-Mg-Zn-Bi-In anodes in 4 M NaOH and 7 M KOH solutions, respectively. Self-corrosion rates are obtained by weight loss measurement in 4 M NaOH and 7 M KOH solutions for 60 min. It was found that the open-circuit potential and self-corrosion rate of Al are higher than those of Al-Mg-Zn-Bi-In in both 4 M NaOH and 7 M KOH solutions. Owing to increase the segregative phases in Al-Mg-Zn-Bi-In by addition of Bi which play the role of activation points, the addition of Bi in to Al-Mg-Zn-Bi-In shifts the open circuit potentials toward more negative values [13].

Fig. 2. here

Table 1. here

Fig. 3 and **Table 2** demonstrate the potentiodynamic polarization curves and corresponding corrosion parameters of Al and Al-Mg-Zn-Bi-In anodes in 4 M NaOH and 7 M KOH solutions, respectively. The more negative corrosion potential of Al-Mg-Zn-Bi-In in alkalinity solutions, which is a mixed electrode potential owing to less thickness of aluminum hydroxide layer and activation of aluminum surface that results in additive alloying elements. For Al-Mg-Zn-Bi-In the corrosion potential in 7 M KOH is more negative than that in 4 M NaOH solutions and the corrosion current density (j_{corr}) in 7 M KOH is less than that in 4 M NaOH solutions.

Fig. 3. here

Table 2. here

Based on the E_{corr} value in **Table 2**, the E_{corr} value increases in the following order: Al-Mg-Zn-Bi-In (KOH) < Al-Mg-Zn-Bi-In (NaOH) < Al (KOH) < Al (NaOH). Also the corrosion current density (j_{corr}) increases in the same order. We can say that the main precipitate phase is $MgZn_2$ particles in Al–Mg-Zn-Bi-In, and the corrosion potential of the bulk $MgZn_2$ is more negative than that of Al [18]. The formation of $MgZn_2$ particles is proved by the EDX analysis that has been followed.

The working mechanisms of alloying elements of Mg, Zn, In and Bi in the alloy are as follows:

Mg: The element of magnesium in such alloys is known to be mainly effecting the mechanical properties of the anode (it used to prevent physical disintegration of the aluminum anode) [19]. In addition, magnesium is an anodic impurity that leads to cathodic polarization (cathodic protection) of the base metal aluminum, resulting in less corrosion rate.

Zn: Zinc can increase the hydrogen evolution potential of the aluminum anode, which results in a decrease in hydrogen evolution and reducing of the aluminum corrosion (Zinc is a cathodic impurity to aluminum) [20].

In: Often times, the initial dissolution of the alloy led to the increase in concentration of In^{3+} ions in the alkaline media. Because indium is cathodic impurity to aluminum and has higher cathodic overvoltage to hydrogen, it is immediately reduced at localized sites and thus will be cathodically protected by the aluminum matrix and will not be dissolved during the anodic dissolution of the aluminum anode [21].

Bi: Considering the metal solidification principle, aluminum with high melting point crystallizes at first. Bismuth with low melting point, is enriched in the liquid of solid-liquid interface during the process of solidification, forming the segregation at the grain boundaries which further activate the alloy to get more negative open circuit potentials [22].

3.2. Electrochemical impedance spectroscopy before discharge

The Nyquist plots of the anodes before discharge in 4 M NaOH and 7 MKOH solutions and fitting of the Nyquist plots are shown in **Fig. 4**. The electrical equivalent circuits for simulating the process are shown in **Fig. 5** and the fitting values of EIS parameters are listed in **Table 3**. To acquire more precious fitting results, the employed capacitance element (C) which indicates the double-layer capacitance is changed by constant phase element (CPE) Q. The Nyquist plots are specified by two capacitive loops at high and low frequencies as well as an inductive loop at low frequencies. The high-frequency capacitive loop in the EIS is the result of charge transfer reaction in the electric double layer which in the case of Al-Mg-Zn-Bi-In in both electrolyte is smaller than that of pure Al. It means that the surface of Al-Mg-Zn-Bi-In is more active than pure Al, so this alloy is superior for use as anode of battery. The being of capacitive loop at low-frequency shows there is a layer of corrosion product film on the anode surface. The low-frequency capacitive loop of Al-Mg-Zn-Bi-In is conspicuous, it indicates that the corrosion products of the alloy had strong adhesion. The high anodic utilization during discharge is partially responsible for the higher R_P, which is well validated by EIS. The low-frequency inductive loop may be shows the pitting of the corroded morphology in **Fig. 6**. It has been reported that the inductive loop is symbol of pitting in the pitting model for Al alloys [23,24]. R_3 and L are the corresponding parameters for pitting. Z-View software has been employed in fitting process (**Table 3**).

Fig. 4. here

Fig. 5. here

Table3. here

The surface morphologies of Al and Al-Mg-Zn-Bi-In after immersion in 4 M NaOH and 7 M KOH solutions for 60 min were obtained by scanning electron microscopy examination. In **Fig. 6B** and **6D**, the morphologies of Al-Mg-Zn-Bi-In in 4 M NaOH and 7 M KOH solutions have pits but they are more flat compare with pure Al in 4 M NaOH and 7 M KOH solutions (**Fig. 6A and 6C**). The EDX analyses of the Al-Mg-Zn-Bi-In alloy are shown in **Fig. 7**. The EDX result of the precipitates in the alloy is mainly comprised of Al, Zn, and Mg elements in **Fig. 7.** The atomic ratio of these elements is about Zn/Mg = 2:1. According to the electronegativity of Zn and Mg elements, it follows that the precipitates may be $MgZn_2$. The presence of pitting corrosion in the images of Al-Mg-Zn-Bi-In may be the result of acting $MgZn_2$ precipitates as corrosion center. It seems that alloying aluminum with particular low melting point elements such In, and Bi, activates it by destructing the passive layer and by distributing evenly on the solid solution of aluminum or in the grain boundaries [25]. These properties combined with high hydrogen evolution overpotential of the alloying elements make Al-Mg-Zn-Bi-In alloy suitable for use as anode of Al-AgO battery.

Fig. 6. here

Fig. 7. here

Aluminum alloying with Mg, Zn, Bi and In, namely Al-Mg-Zn-Bi-In anode possesses the more negative potential, activated surface and the less self-corrosion rate. Based on the above analysis, in contrast to pure Al, Al-Mg-Zn-Bi-In could be used in Al-AgO battery as anode.

3.3. Battery performance

Fig. 8 shows the discharge behavior of Al-AgO battery at current densities of 50 mA cm^{-2}. The cell potential falls quickly in the early discharging time, which is happened by the battery internal resistance. It should be noted that the cell potential of the battery with Al-Mg-Zn-Bi-In anode in 7 M KOH solution is close to 2.05 V and fluctuation of the alloy in NaOH solution is clearly lowest compared with others.

Favored electrolytes for Al-AgO batteries are 4 M NaOH and 7 M KOH, which relate to their peak electrolytic conductivities. The peak electrolytic conductivity of 7 M KOH at 0.7 S cm^{-1}, is higher than that of 4 M NaOH (0.39 S cm^{-1}). The solubility limit of the reaction product, $Al(OH)_4^-$, is also higher in 7 M KOH at 6 g per 100 g of electrolyte relative to 4 g per 100 g of electrolyte for a 4 M NaOH solution. This is an important regard for Al-AgO batteries using static electrolytes, as when the saturation level for $Al(OH)_4^-$ is achieved, it precipitates out as $Al(OH)_3$ [26]. Mentioned items resulted in different performance of the two electrolytes.

Fig. 8. here

Table 4 summarizes the performance of the above batteries at 50 $mAcm^{-2}$. As show in **Table 4**, the battery with Al-Mg-Zn-Bi-In anode in 7 M KOH solution reveals the highest anodic utilization compared with the others in alkaline solutions. The anodic utilization of Al-Mg-Zn-Bi-In in KOH is more than that of in NaOH solution. In Al-AgO battery with alkaline electrolyte, in accord with reaction (1) and (2), anodic dissolution of aluminum creates $Al(OH)^{4-}$ ions, which activates the surface of anode. The anodic process of aluminum oxidation is combined with the cathodic process of water reduction according to the reaction (2), which acts as secondary cathode and reduce the columbic efficiency of anode.

$$Al + 3OH^- \rightarrow Al(OH)_3 \downarrow + 3e^- \qquad (1)$$

$$Al(OH)_3 + OH^- \rightarrow Al(OH)_4^- \qquad (2)$$

$$2H_2O + 2e^- \rightarrow H_2 + 2OH^- \qquad (3)$$

Table 4. here

3.4. Electrochemical impedance spectroscopy after discharge

The Nyquist plots of the anodes after discharge in 4 M NaOH and 7 MKOH solutions and fitting of the Nyquist plots are shown in **Fig. 9**. The electrical equivalent circuits for fitting the process are shown in **Fig. 5** and the fitting values of EIS parameters are listed in **Table 3**. The Nyquist plots are characterized by two capacitive loops at high and low frequencies as well as an inductive loop at low frequencies. Compared to EIS before discharge, the capacitive loops especially for Al are minimized and subsequently the charge transfer resistance decreased. The low-frequency loop of Al-Mg-Zn-Bi-In is the biggest, it mentions the corrosion product film is not easy to separate, it increases the corrosion resistance of the alloy. In the case of Al-Mg-Zn-Bi-In the low-frequency capacitive loop in the EIS may be the result of a dissolution-precipitation from In and Zn ions.

Fig. 9. here

4. Conclusions

In conclusion, we investigated the corrosion behavior and discharge performance of Al, Al-Mg-Zn-Bi-In anodes in 4 M NaOH and 7 M KOH electrolytes. The results show that compared with Al, Al-Mg-Zn-Bi-In anode has excellent electrochemical performance and lower self-corrosion rate. The corrosion potential and the self-corrosion measurement of Al-Mg-Zn-Bi-In in 7 M KOH are -1.988 V and 138.635 mmpy, respectively. Using Al-Mg-Zn-Bi-In as anode could improve the performance of Al-AgO battery, and reduce the problem of severe self-corrosion and passivation. At a current density of 50 mA cm^{-2}, the operate voltage of Al-AgO battery with Al-Mg-Zn-Bi-In anode in 7 M KOH electrolyte is 2.04 V, and the anodic utilization is 69.95 %.

5. Acknowledgment

This work was sponsored by the Bu Ali Sina University which is gratefully appreciated.

6. References

[1] Z.A. Zhuk, E.A. Sheindlin, V.B. Kleymenov, I.E. Shkolnikov, Y.M. Lopatin, J. Power Sources 157 (2006) 921-926.

[2] Z. Ma, X. Li, J Solid State Electrochem 15 (2011) 2601–2610.

[3] G. E. Anderson, Middletown, R.I., U.S. Patent No. 3953239 (1976).

[4] R. Narayan, K. P. Sheriff, Key Eng Mat. 20 (1987) 295-303.

[5] S. Gudic, I. Smoljko, M. Kliskic, Electrochim. Acta 50 (2005) 5624-5632.

[6] M.A. Amin, E.R. Abd, S. Sayed, E.F. Essam, R.S. Mahmoud, N.M. Abbas, Electrochim. Acta 54 (2009) 4288-4296.

[7] S.E.A. Zein, A.Q. Saleh, J. Appl. Electrochem. 34 (2004) 331-339.

[8] W. Xiong, G.T. Qi, X.P. Guo, Z.L. Lu, Corros. Sci. 53 (2011) 1298-1303.

[9] J. Ma, J. Wen, J. Gao, Q. Li, Electrochim. Acta 129 (2014) 69-75.

[10] I. Herraiz-Cardona, E. Ortega, V. Perez-Herranz, Electrochim, Acta 56 (2011) 1308-1315.

[11] S.A. Mideen, M. Ganesan, M.A. Athan, K.B. Sarangapani, V. Balaramachandran, V. Kapali, S.V. Iyer, J. Power Sources 27 (1989) 235-244.

[12] Q. Li, N. J. Bjerrum , J. Power Sources 110 (2002) 1-10.

[13] J. Gao, J. Wen, J. He, Adv. Mat. Res. 800 (2013) 488-491.

[14] C.B. Breslin, W.M. Carroll, Corros. Sci. 34 (1993) 327–341.

[15] S.B. Saidman, J.B. Bessone, J. Appl. Electrochem. 27 (2003) 731–736.

[16] A.G. Munoz, S.B. Saidman, J.B. Bessone, Corros. Sci. 44 (2002) 2171–2177.

[17] W. Bohnstedt, J. Power Sources 5 (1980) 245-253.

[18] M. Jingling, W. Jiuba, Corros. Sci. 51 (2009) 2115–2119.

[19] J.R. Davis (Ed.), ASM Speciality Handbook, ASM International, Davis & Associates, 1993, ISBN 0-87170-496-X.

[20] Y. Tang, L. Lu, H. W. Roesky, L. Wang, B. Huang, J. Power Sources 138 (2004) 313–318.

[21] M. C. Reboul, Ph Gimenez, and J. J. Rameau, Corrosion 40 (1984) 366-371.

[22] J. He, J. Wen, X. Li, G. Wang, C. Xu, Trans. Nonferrous Met. Soc. China 21 (2011) 1580-1586.

[23] F. Mansfeld, Electrochim. Acta 38 (1993) 1891-1897.

[24] G. A. Zhang, Y. F. Cheng, Corros. Sci. 51 (2009) 1589-1595.

[25] J. Ma, J. Wen, J. Gao, Q. Li, J. Power Sources 253 (2014) 419-423.

[26] D.R. Egan, C. Ponce de León, R.J.K. Wood, R.L. Jones, K.R. Stokes, F.C. Walsh, J. Power Sources 236 (2013) 293-310.

Figure captions

Fig. 1. The procedure of preparing optimal AgO cathode (A) electrode grid before silver-plating (B) electrode grid after silver-plating (C) active AgO electrode.

Fig. 2. Open-circuit potential vs time for Al and Al-Mg-Zn-Bi-In for half-cell in 4 M NaOH and 7 M KOH solutions.

Fig. 3. Potentiodynamic polarization curves for Al and Al-Mg-Zn-Bi-In measured in 4 M NaOH and 7 M KOH solutions.

Fig. 4. Nyquist plots of the Al and Al-Mg-Zn-Bi-In before discharge in 4 M NaOH and 7 M KOH solutions.

Fig. 5. Equivalent circuits compatible with the Nyquist plots: Al (a) and Al-Mg-Zn-Bi-In (b).

Fig. 6. SEM images of anodes after 60 min immersion times: Al in 4 M NaOH and 7 M KOH solutions (A), (C); Al-Mg-Zn-Bi-In alloy in 4 M NaOH and 7 M KOH solutions (B),(D), respectively.

Fig. 7. EDX results of Al-Mg-Zn-Bi-In alloy in (A) NaOH and (B) KOH solutions obtained from the precipitates in **Fig. 6**.

Fig. 8. Discharge behavior of Al-AgO battery at current densities of 50 mA cm^{-2} in 4 M NaOH and 7 M KOH electrolytes.

Fig. 9. Nyquist plots of the Al and Al-Mg-Zn-Bi-In obtained after discharge at current densities of 50 mA cm^{-2} for 20 min in 4 M NaOH and 7 M KOH solutions.

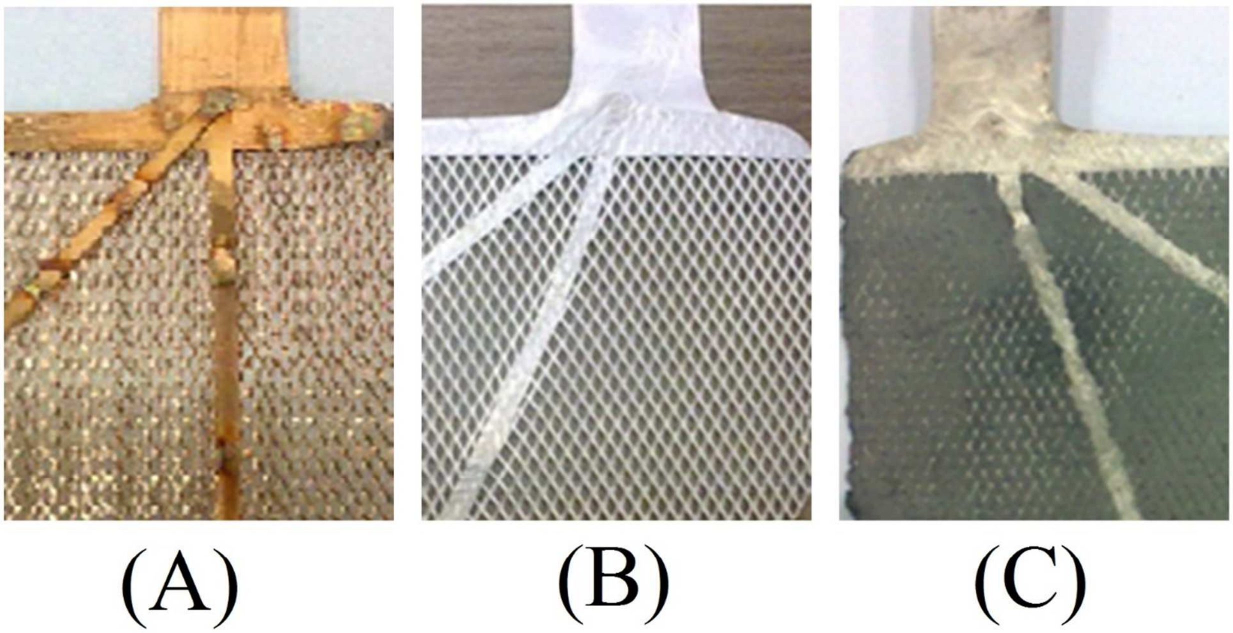

Fig. 1.

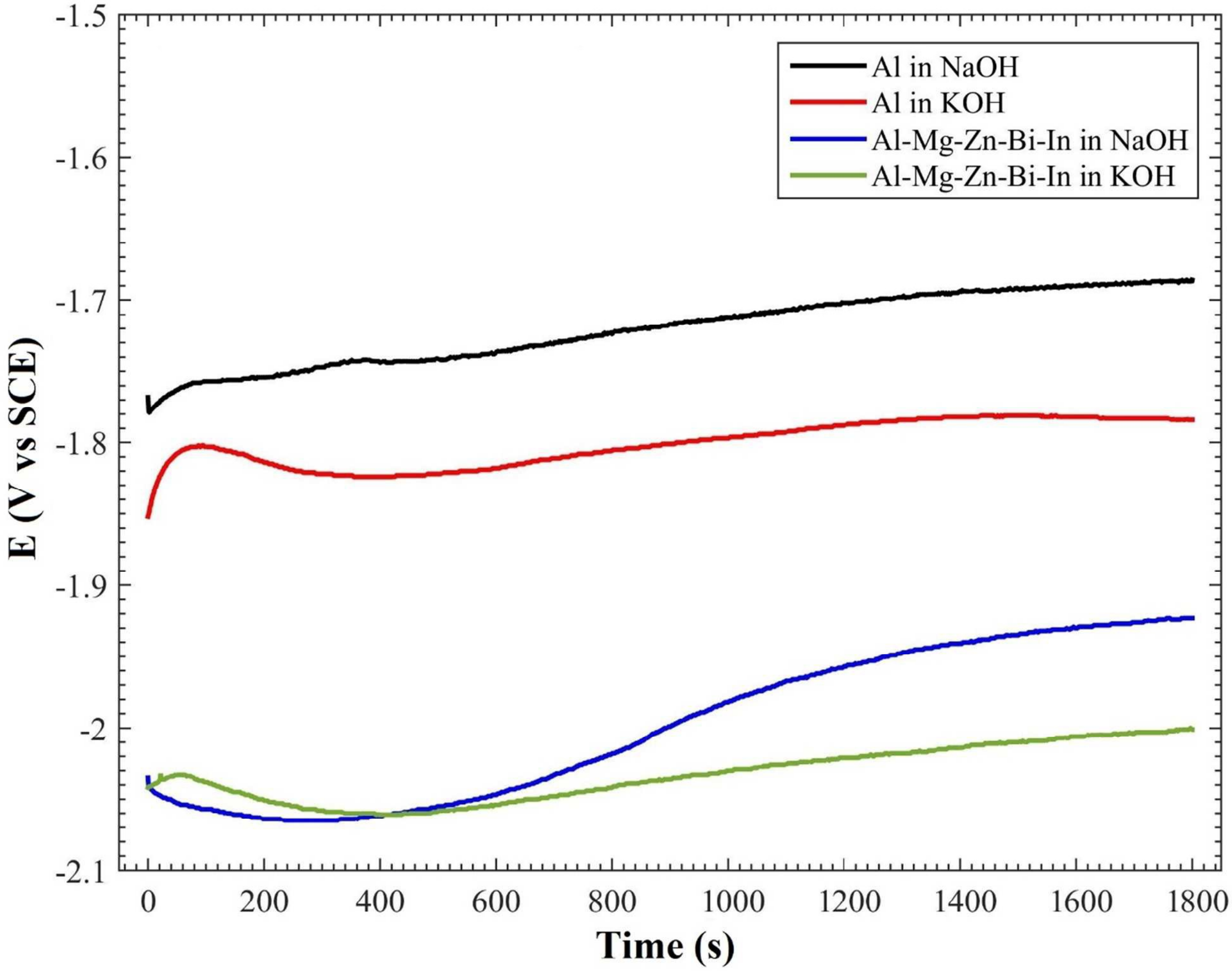
-1.5
-1.6
-1.7
-1.8
-1.9
-2
-2.1
E (V vs SCE)
0
200
400
600
800
1000
1200
1400
1600
1800
Time (s)
Al in NaOH
Al in KOH
Al-Mg-Zn-Bi-In in NaOH
Al-Mg-Zn-Bi-In in KOH

Fig. 2.

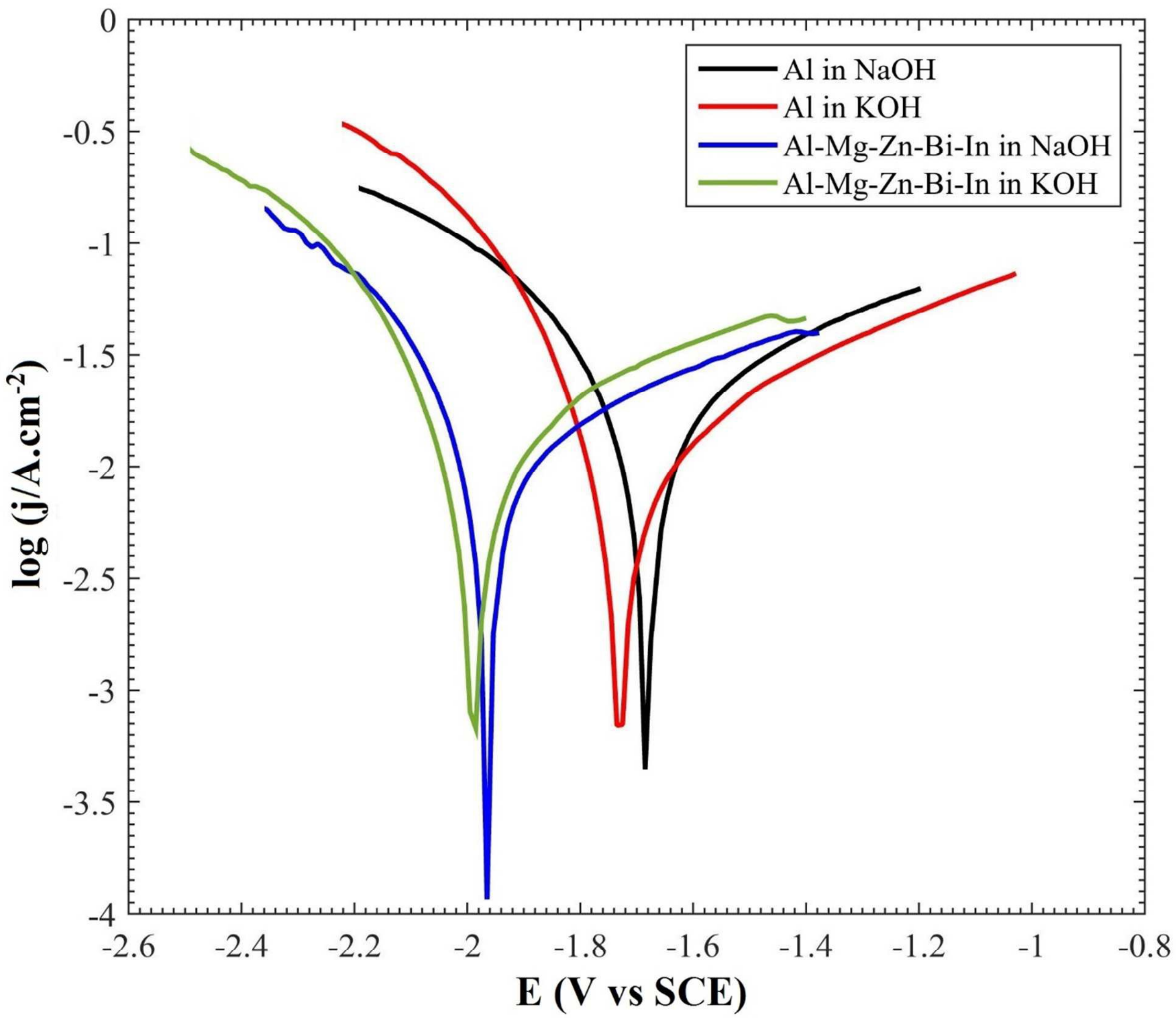

Al in NaOH
Al in KOH
Al-Mg-Zn-Bi-In in NaOH
Al-Mg-Zn-Bi-In in KOH
0
-0.5
-1
-1.5
-2
-2.5
-3
-3.5
-4
log (j/A.cm-2)
-2.6
-2.4
-2.2
-2
-1.8
-1.6
-1.4
-1.2
-1
-0.8
E (V vs SCE)

Fig. 3.

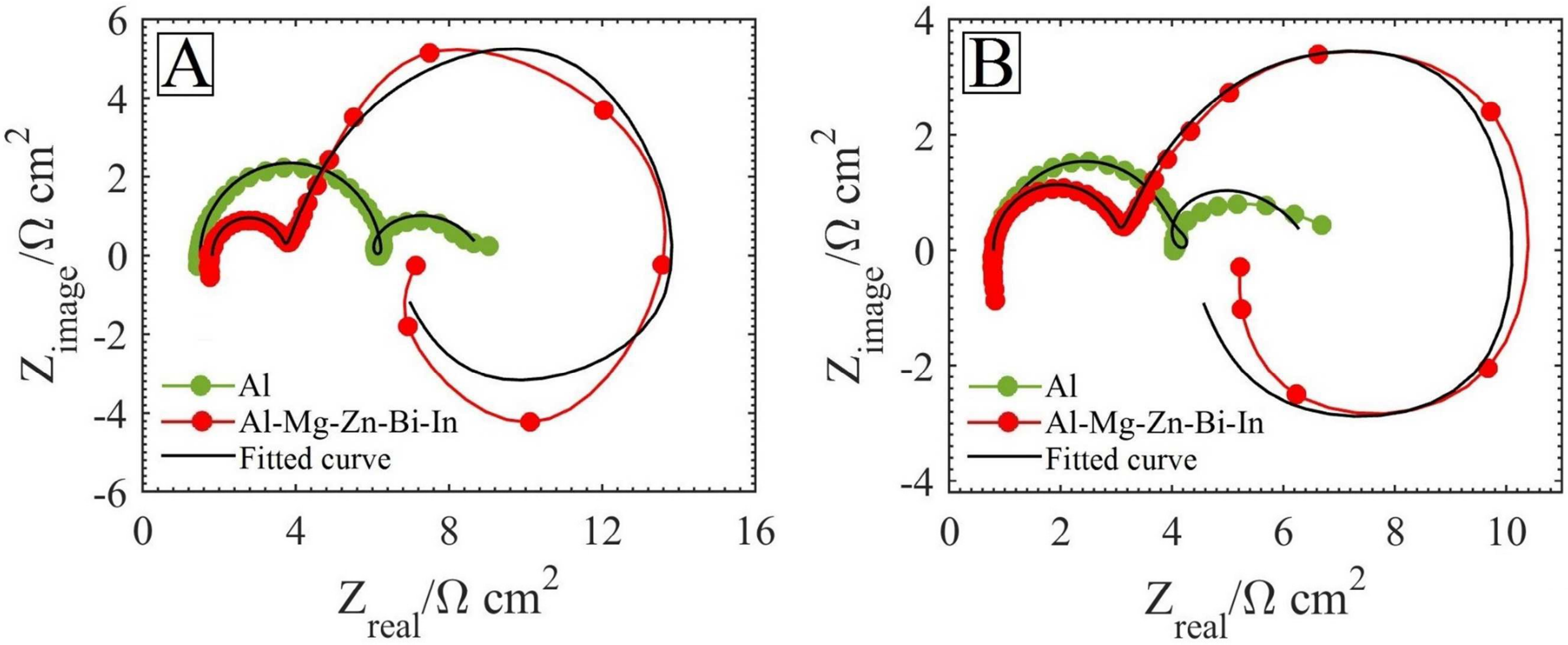
A
B
Z_image/Ω cm²
Z_real/Ω cm²
6
4
2
0
-2
-4
-6
0
4
8
12
16
2
6
10
Al
Al-Mg-Zn-Bi-In
Fitted curve

Fig. 4.

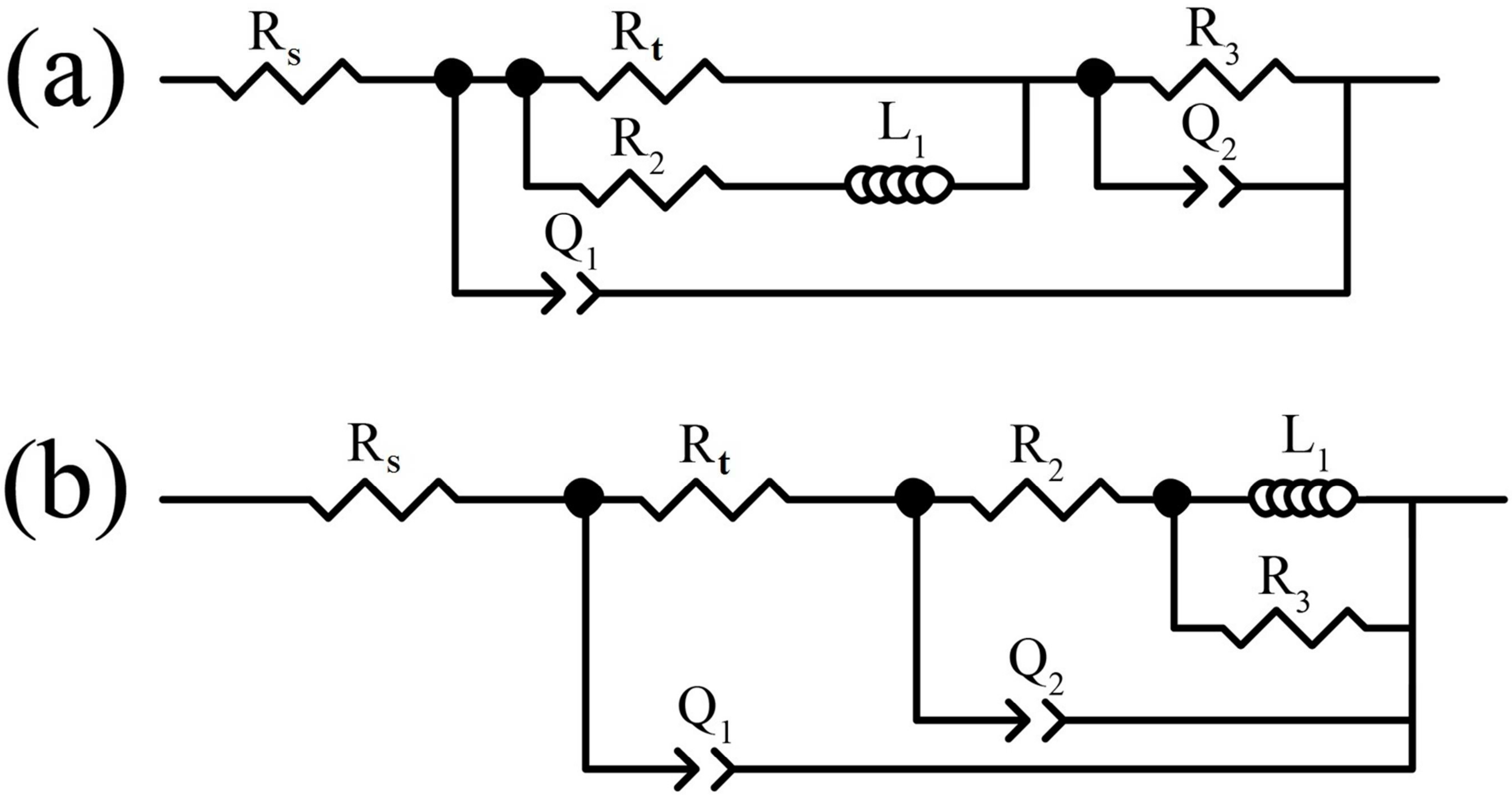

Fig. 5.

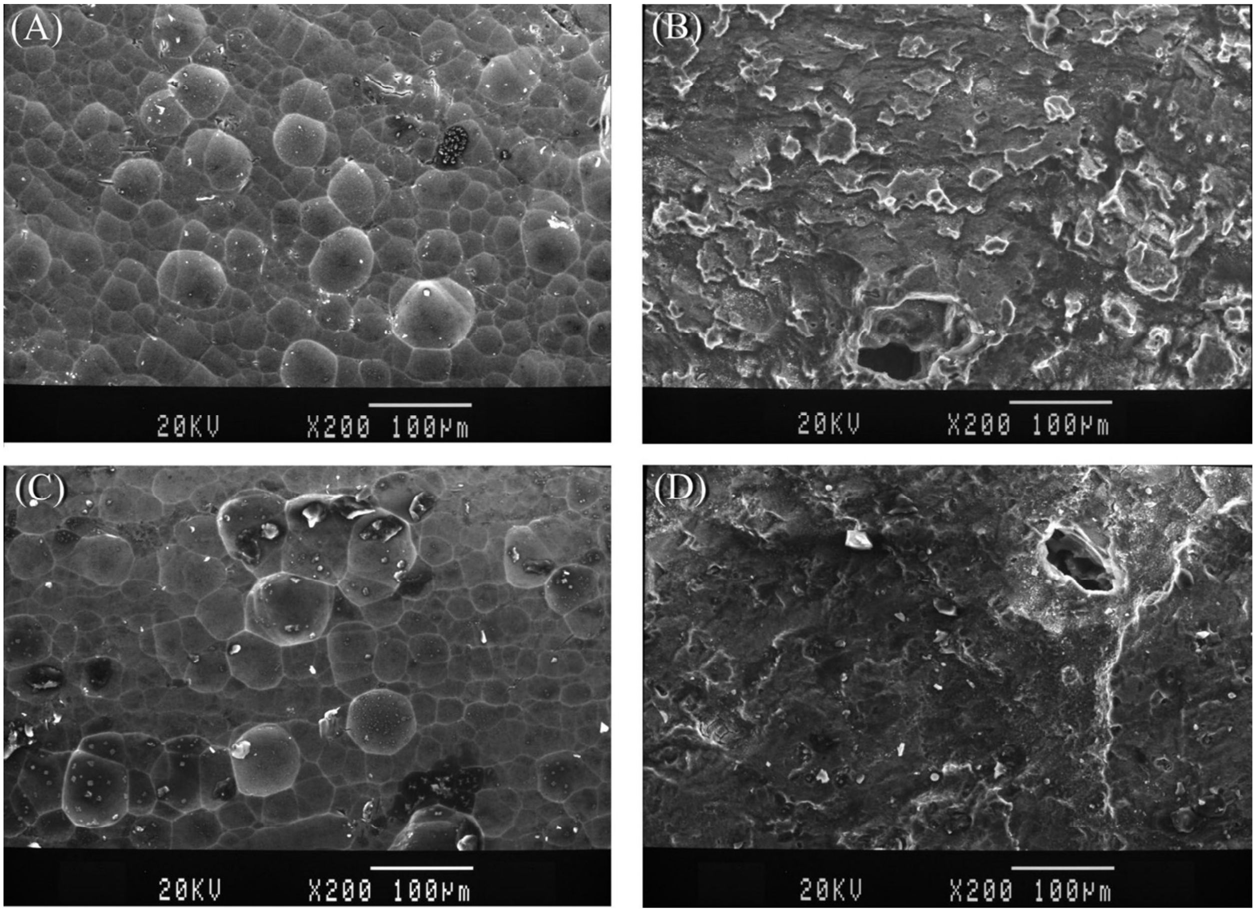
(A)
20KV X200 100µm
(B)
20KV X200 100µm
(C)
20KV X200 100µm
(D)
20KV X200 100µm

Fig. 6.

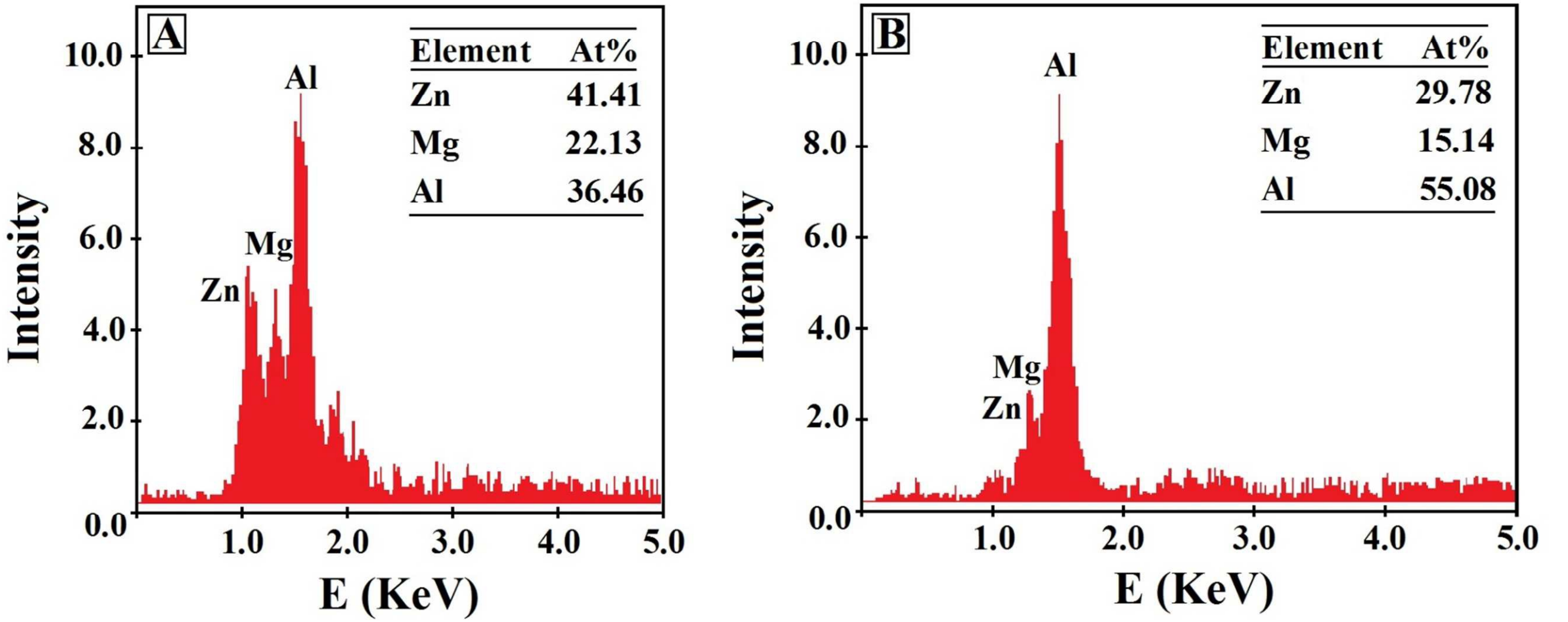
A
Intensity
E (KeV)
Zn
Mg
Al
0.0
2.0
4.0
6.0
8.0
10.0
1.0
2.0
3.0
4.0
5.0
Element At%
Zn 41.41
Mg 22.13
Al 36.46
B
Intensity
E (KeV)
Zn
Mg
Al
0.0
2.0
4.0
6.0
8.0
10.0
1.0
2.0
3.0
4.0
5.0
Element At%
Zn 29.78
Mg 15.14
Al 55.08

Fig. 7.

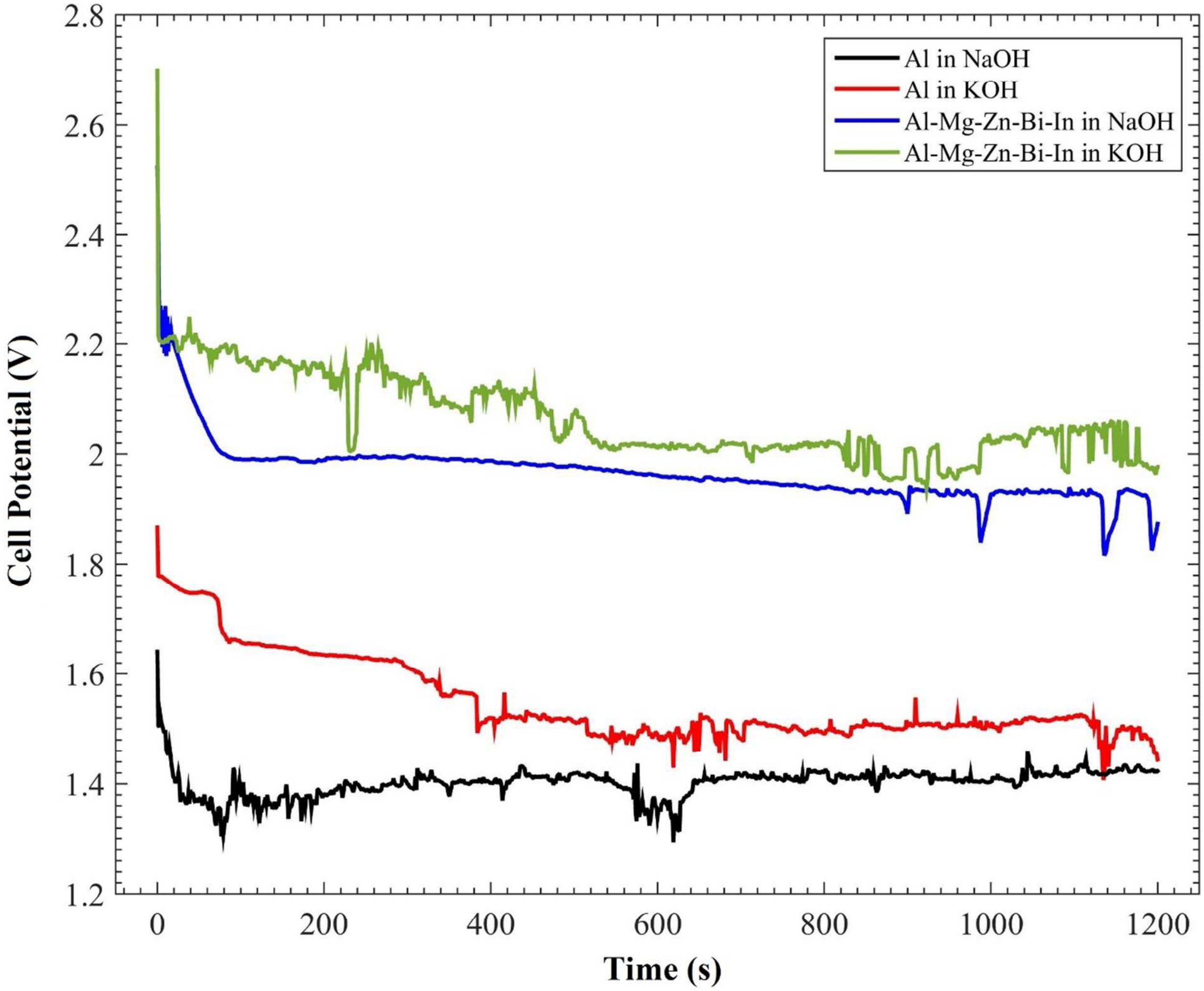
Cell Potential (V)
2.8
2.6
2.4
2.2
2
1.8
1.6
1.4
1.2
Time (s)
0
200
400
600
800
1000
1200
Al in NaOH
Al in KOH
Al-Mg-Zn-Bi-In in NaOH
Al-Mg-Zn-Bi-In in KOH

Fig. 8.

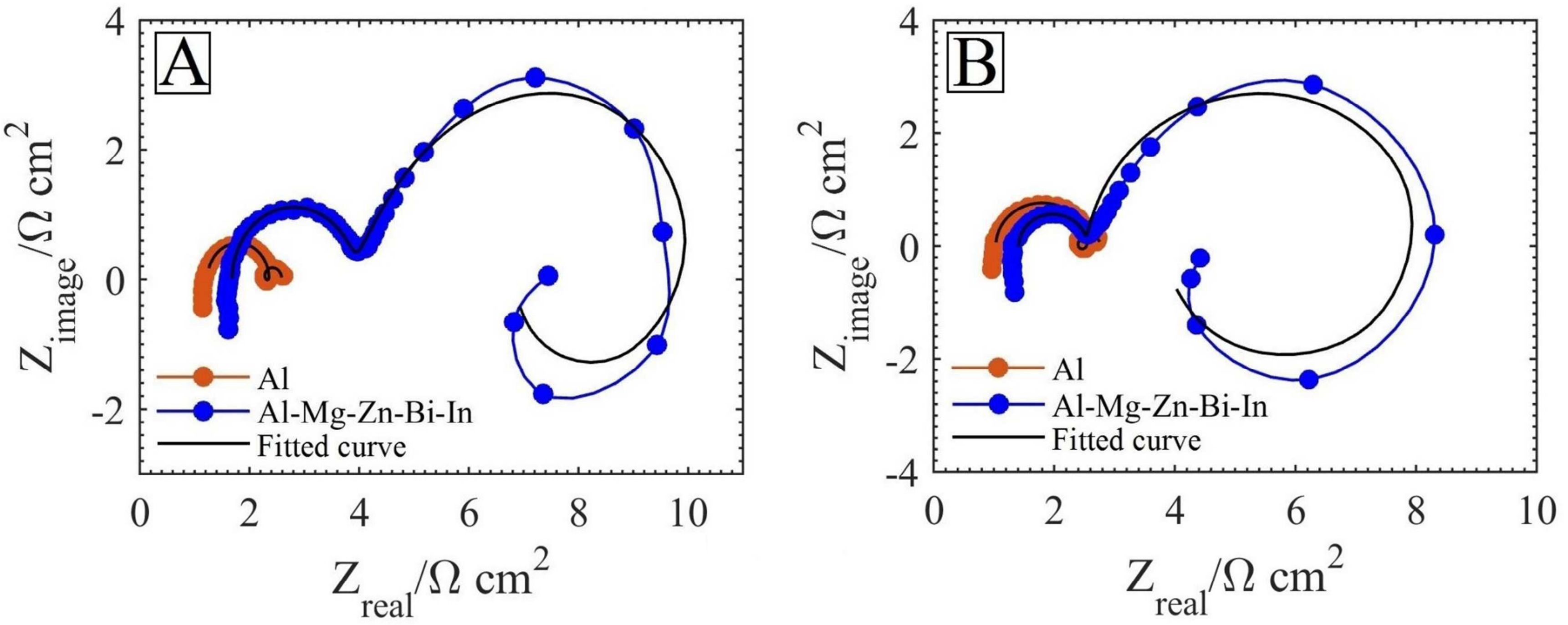
A
B
4
2
0
-2
-4
0
2
4
6
8
10
$Z_{image}/\Omega\ cm^2$
$Z_{real}/\Omega\ cm^2$
Al
Al-Mg-Zn-Bi-In
Fitted curve

Fig. 9.

Table 1. Self-corrosion rates of Al and Al−Mg−Zn−Bi−In in 4 M NaOH and 7 M KOH solutions.

Anodes	Solutions	Weight loss/mg	Corrosion rate/mg cm^{-2} h^{-1}	Corrosion rate/ mmpy
Al	4 M NaOH	63.5	17.162	556.811
Al-Mg-Zn-Bi-In	4 M NaOH	24.6	5.187	168.289
Al	7 M KOH	40.0	10.810	350.724
Al-Mg-Zn-Bi-In	7 M KOH	20.3	4.273	138.635

Table 2. Corrosion parameters of Al and Al−Mg−Zn−Bi−In in 4 M NaOH and 7 M KOH solutions.

Anodes	Solutions	E_{corr} (V vs SCE)	j_{corr} (mA cm^{-2})	R_p (Ω cm^2)
Al	4 M NaOH	-1.681	20.515	6.923
Al-Mg-Zn-Bi-In	4 M NaOH	-1.963	7.127	9.709
Al	7 M KOH	-1.738	10.214	8.265
Al-Mg-Zn-Bi-In	7 M KOH	-1.988	6.398	8.376

Table 3. The area-normalized values of the elements in equivalent circuits of **Fig. 5** fitted in the Nyquist plots of **Fig. 4** and **Fig. 9.**

Electrolytes	4 M NaOH				7 M KOH			
	Al		Al-Mg-Zn-Bi-In		Al		Al-Mg-Zn-Bi-In	
	Before discharge	After discharge	Before discharge	After discharge	Before discharge	After discharge	Before discharge	After discharge
R_s (Ω.cm^2)	1.50	1.23	1.82	1.68	0.68	1.03	0.80	1.41
Q_1 (F.cm^{-2})	14.3μ	20μ	52.1μ	56.7μ	11.2μ	17.1μ	87.2μ	95.6μ
n_1 ($0<n<1$)	1	0.99	1	1	0.91	1	1	1
R_t (Ω.cm^2)	4.68	1.12	1.90	2.22	3.83	1.53	2.26	1.12
L_1 (H cm^2)	0.20	0.014	2.27	0.98	0.386 m	0.014	1.59	1.34
R_2 (Ω.cm^2)	26.91	0.81	11.41	6.29	8.37	10.8	7.24	6.98
Q_2 (F.cm^{-2})	0.060	0.013	0.029	0.027	0.072	0.078	0.040	0.023
n_2 ($0<n<1$)	0.70	0.98	0.80	0.74	0.71	0.99	0.79	0.92
R_3 (Ω.cm^2)	3.41	0.88	18.24	7.23	2.60	0.39	11.97	5.05
R_p (Ω.cm^2)	8.09	2	13.31	8.51	6.43	1.92	9.5	8.1

Table 4. The discharge performance of Al-AgO battery with Al and Al-Mg-Zn-Bi-In at current densities of 50 mAcm^{-2} for 20 min in 4 M NaOH and 7 M KOH solutions.

electrolytes	Cell potential (V)		Anodic utilization (%)	
	Al	Al-Mg-Zn-Bi-In	Al	Al-Mg-Zn-Bi-In
4 M NaOH	1.41	1.96	58.91	65.84
7 M KOH	1.49	2.04	62.18	69.95